

Applications of the DNS CONV-3D Code for Simulations the Matis-H experiment

Vladimir V. Chudanov, Anna E. Aksenova, Valerii A. Pervichko

Abstract — In this paper, we present the results of the CONV-3D code application for modeling the Matis-H experiment (Korea) on water coolant flow around the test assembly with different types of grid spacers. A satisfactory coincidence of numerical predictions with the experiment, in particular, on the distribution of average velocity and rms its depending on the coordinate, is demonstrated. The calculations performed allow recommending the use of the CONV-3D code of the DNS class, which has a high predictive capacity, for the calculation coolant flow around the fuel assembly with different types of grid spacers.

Keywords — DNS, CFD, CONV-3D, fuel assembly, grid spacer.

I. INTRODUCTION

The relevance in the development of new computational methods for calculating heat and hydrodynamics in fuel assemblies on high-performance cluster machines was noted at all recent international conferences and symposia on nuclear power [1]. In the context of the development of radiation safety standards of the IAEA there is a need for a multidimensional description of the processes of heat and hydrodynamics for different emergency modes, taking into account the current level of development of computer technology and numerical CFD methods. A common task is to develop new multidimensional computational tools for adequate analysis of a wide range of heat and hydrodynamic processes in reactor plants. Their subsequent implementation in the developed codes of the nuclear industry will raise to a qualitatively new level of safety justification, design support, necessary for the safe operation of working and promising nuclear power plants.

The heat transfer problem in a fuel assembly is relevant in connection with interchannel heat exchange in the reactor plants. To ensure a sufficient level of turbulence flow, various turbulators and grid spacers are used. Under reactor conditions, it is not possible to estimate a degree of turbulence influence on the level of interchannel heat exchange.

V. V. Chudanov is with the Nuclear Safety Institute (IBRAE) of Russian Academy of Sciences, 52, Bolshaya Tulsкая street, Moscow, 115191, Russia (corresponding author to provide phone: +7-495-955-22-34; e-mail: chud@ibrae.ac.ru).

A. E. Aksenova is with the Nuclear Safety Institute (IBRAE) of Russian Academy of Sciences, 52, Bolshaya Tulsкая street, Moscow, 115191, Russia (corresponding author to provide phone: +7-495-955-22-34; e-mail: aks@ibrae.ac.ru).

V. A. Pervichko is with the Nuclear Safety Institute (IBRAE) of Russian Academy of Sciences, 52, Bolshaya Tulsкая street, Moscow, 115191, Russia (corresponding author to provide phone: +7-495-955-22-34; e-mail: valper@ibrae.ac.ru).

Therefore, numerical modeling of such problems with the help of CFD codes is relevant. This article presents the results of modeling using the CFD code CONV-3D of DNS class, written from the first principles. This is a significant advantage compared to the traditional RANS codes, which require the selection of turbulence models and corresponding coefficients for the studied flow class. For codes of DNS type, this issue has been resolved, which reduces uncertainty and evaluation time. And the presence of supercomputers can significantly improve not only the accuracy of calculations, but also the speed in the evaluation of results and decision-making. This paper presents the results of simulation of the experiment with water coolant. But since the code is written from the first principles, it can be used, without limitation of generality, to solve tasks, in particular, for the reactor facility with sodium coolant.

For the simulation of the thermalhydraulic processes in different type reactors CFD code CONV-3D of the DNS class has been developed [2—4]. This code has ideal scalability and is very effective for calculations on high performance cluster computers. The code has been validated on the set of analytical tests and experiments in a wide range of Rayleigh and Reynolds numbers, in particular, at extremely small Prandtl numbers [5—7].

The article presents the results of the CONV-3D code application for simulation of Matis-H experiment used for hydraulic test in a bundle of rods with different types of grid spacers under normal pressure and temperature. A good agreement between the numerical predictions and experiment was demonstrated.

The performed calculations allow recommending the use of the CONV-3D code of the DNS class, which has a high predictive capacity, for the calculation of the coolant flow around the fuel assembly with different types of grid spacers.

II. PECULIARITIES OF MODELING MATIS TEST FACILITY

The features of the Matis experiment (Korea) are detailed in [8]-[9]. Here we will briefly focus on the features taken into account when modeling. It was a blind test conducted by KAERI (Korea Atomic Energy Research Institute), which was attended by over 20 countries.

A schematic of the test facility, which is located at the Daejeon, Korea, is illustrated in figure 1.

This cold loop test facility, with the acronym MATIS-H (Measurement and Analysis of Turbulent Mixing in Subchannels – Horizontal), is used to perform hydraulic tests in a rod bundle array at normal pressure and temperature conditions.

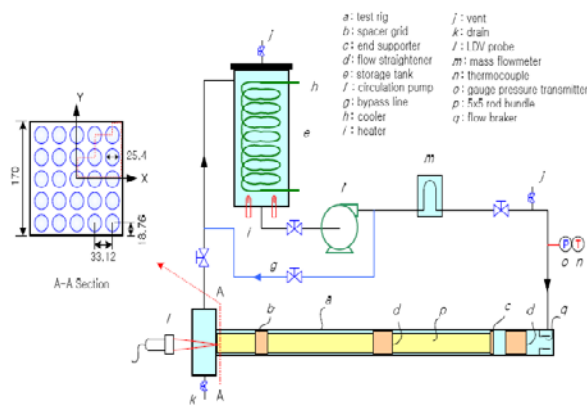


Fig. 1 schematic of MATiS-H test facility

The rig consists of a water storage tank (*e*), a circulation pump (*f*) and a test section (*a*). The volume of the water storage tank and the maximum flow rate of the circulation pump are 0.9 m^3 and $2 \text{ m}^3/\text{min}$, respectively. The flow rate in the loop during operation is controlled by adjusting the rotational speed of the pump, and the loop coolant temperature is also accurately maintained within a range of $\pm 0.5^\circ\text{C}$ by controlling the heater (*i*) and the cooler (*h*) in the water storage tank. For monitoring and controlling the loop parameters (flow rate, pressure and temperature), a mass flowmeter (*m*), a gauge pressure transmitter (*o*) and a thermocouple (*n*) are installed at the inlet to the test section.

The test section (*a*) consists of a 5×5 rod bundle array (*p*) installed in a horizontal position. Section A-A in figure 1 shows the cross-section of the rod bundle in the square duct ($170 \times 170 \text{ mm}$), comprising 25 rods of 25.4 mm outer diameter. The rods are deliberately selected to have a 2.67 times larger diameter than the real size (9.5 mm) of a fuel rod in order to improve the measurement resolution. The rod and the wall pitches are set at 33.12 mm and 18.76 mm , respectively, consistent with the increase in rod diameter. Consequently, the hydraulic diameter of the channel cross-section (DH), which considers the flow area and the wetted perimeter in a square duct including a 5×5 rod bundle, is 24.27 mm . The test section has been installed in a horizontal position for convenience, there being no buoyancy-induced effects.

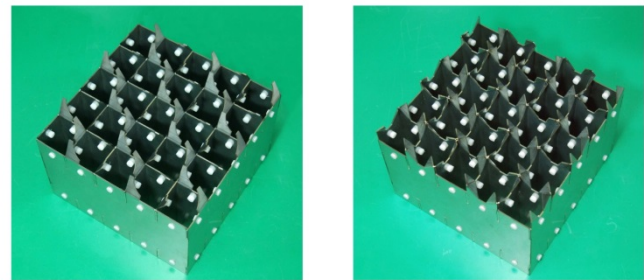
Water is supplied from the storage tank to the inlet to the test section by pump operation. The flow in the square duct first encounters a fixed flow straightener (*d*), which comprises many small square channels in order to produce a uniform flow profile across the duct, without swirl. Downstream, the flow encounters the 5×5 rod bundle, producing a developing flow along the rods. Further downstream, there is a second flow straightener (*d*), placed across the rod bundle, to redistribute the profile again to one of uniform flow. From this location, the flow advances to the spacer grid (*b*), once more changing to a developing flow.

There is sufficient distance ($> 90 DH$) between the 2nd flow straightener and the spacer grid for the flow to be expected to

be fully developed. With this inlet flow condition at the upstream side of the spacer grid, the flow on the downstream would be totally redistributed by the complicated vane arrangement of the spacer grid geometry.

The total length of test section is 4970 mm , the most part made up of the square duct containing the 5×5 rod bundle. At the far upstream end, the inlet pipe (diameter 105 mm) is attached vertically. Once the flow has been turned through 90° , in which a flow breaker is positioned to make the flow profile less biased, it encounters the first of the flow straighteners, which is 150 mm long. A further 250 mm downstream is the start of the rod bundle. This extends over 3863 mm , and is fixed by support grids at both ends. The second flow straightener is located at a specified distance from the inlet plane of the spacer grid. The spacer grid dramatically enhances turbulent mixing in the sub-channels of the bundle due to the attached vanes at its downstream side.

Visually, the grid spacers described in the text above have a view as in figure 2.



(a) Split-type spacer grid

(b) Swirl-type spacer grid

Fig. 2 test spacer grids used in this experiment

De-mineralized water is used as the working fluid in the experiment, the water temperature during operation being maintained at 35°C , at ambient pressure.

The enclosing material of the test section is made of stainless steel and acrylic. The upper plates of the square duct are made of acrylic plate, and the other parts constructed of stainless steel. All components included in the test section, i.e. the 5×5 rod bundle array, the spacer grid and flow straighteners, are made from stainless steel.

A flow profile at $90 DH$ has been given for use as the inlet boundary condition for the CFD calculations.

To measure details of the flow profile at $90 DH$, an additional experiment has been performed using a LDA system as illustrated in Fig. 3.

Here, the flow straightener is placed $90 DH$ upstream of the A-A measurement section, but with the spacer grid removed, as shown in Fig. 3(b). For the measurements of the axial velocity profile, the LDA probe is placed at the side wall of the test rig as shown in Fig. 3(a).

The measurements are restricted to the gap regions in the inner subchannels due to the blockage of the beam caused by the rod structures in the 5×5 rod bundle array. Therefore, the measurement region was taken with the three gap regions at a quadrant section marked in red in Fig. 3(c).

The axial (z-direction) velocities, and their turbulence properties in terms of the turbulence intensity, have been measured simultaneously using the above LDA set-up.

The available measurement region in the quadrant section in Fig. 3(c) is comprised of three gaps (i.e. lower gap, middle gap and upper gap). Fig. 3(d) shows the zoomed locations of the measurement lines at these three intervals in a quarter section, as shown in figure 1 (a-a section), based on normalized scales.

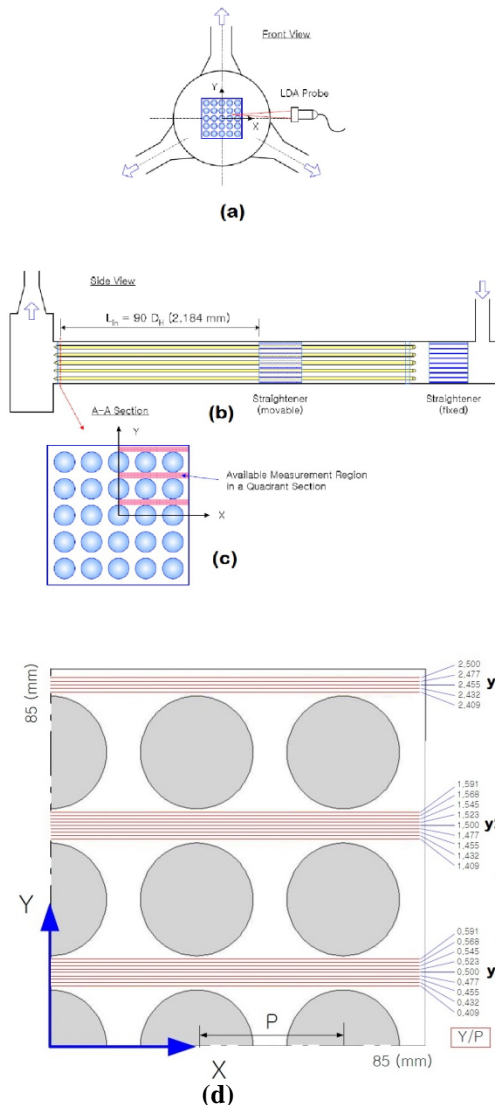


Fig. 3 axial velocity (W) measurements (in 1/4 section) and LDA measurement trajectories in the quadrant section

III. NUMERICAL PREDICTIONS

The results for a split-type grid spacer will be presented first. The results are presented by cross-sections in the following sequence: 0.5DH, 1.0 DH, 4.0DH, respectively. Each section shows the positions for y1 and y2 of the averaged velocity U, depending on the time. All results are reported in comparison with data of KAERI [9].

Figures 4-9 show the results of numerical predictions for a split-type grid spacer. In all figures, the results of numerical

predictions using CONV-3D code are shown as a solid line. Experimental data [9] in all figures are shown by dotted line (•••).

As can be seen from figures 4-9, the coincidence of numerical predictions with the experiment is satisfactory. For the averaged velocity V a satisfactory coincidence in the same positions y1 and y2 is obtained also. But without limiting the generality, we do not give these graphs here.

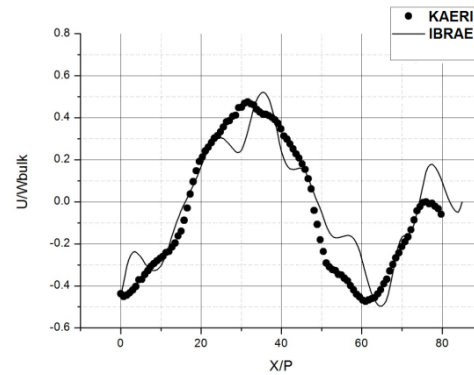


Fig.4 average U velocity in the cross-section of 0.5 DH in the position y1

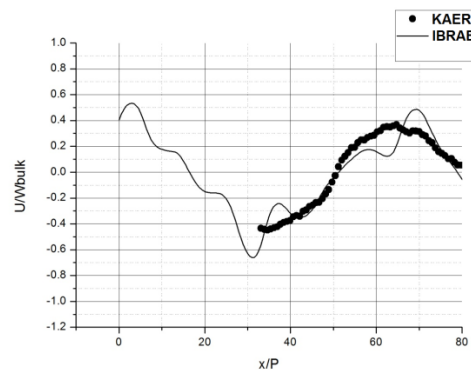


Fig. 5 average U velocity in the cross-section of 0.5 DH in the position y2

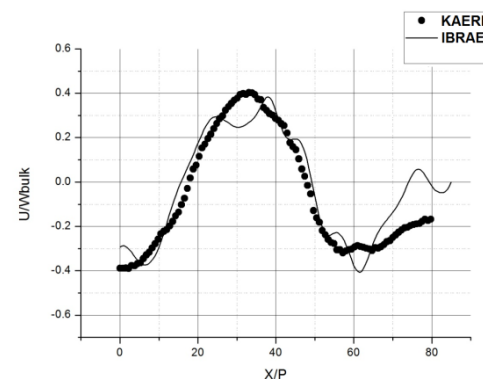


Fig. 6 average U velocity in the cross-section of 1.0 DH in the position y1

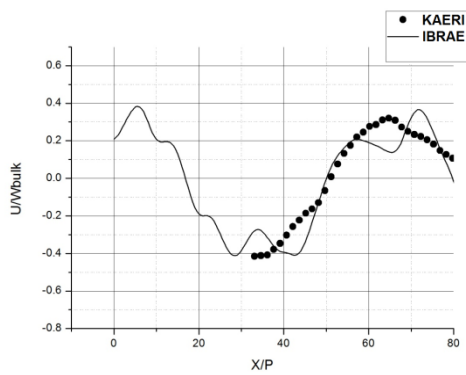


Fig. 7 average U velocity in the cross-section of 1.0 DH in the position y2

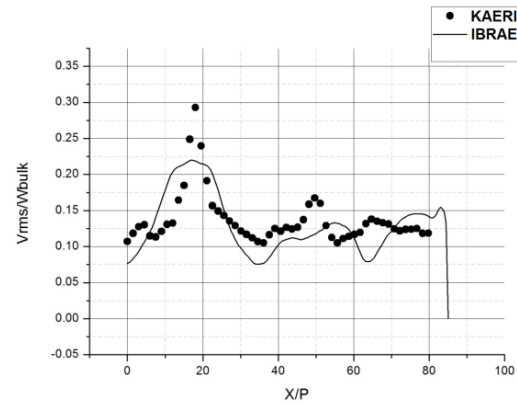


Fig. 10 Rms V velocity in the cross-section of 4.0 DH in the position y1

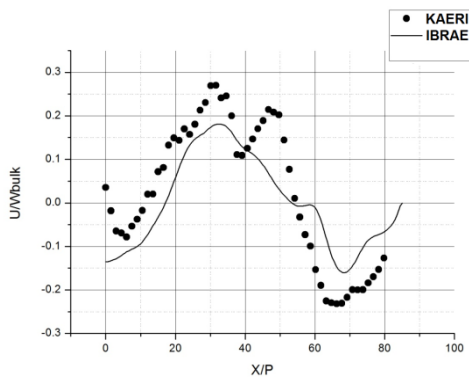


Fig. 8 average U velocity in the cross-section of 4.0 DH in the position y1

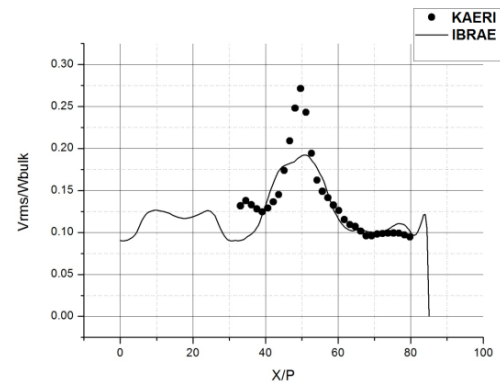


Fig. 11 Rms V velocity in the cross-section of 4.0 DH in the position y2

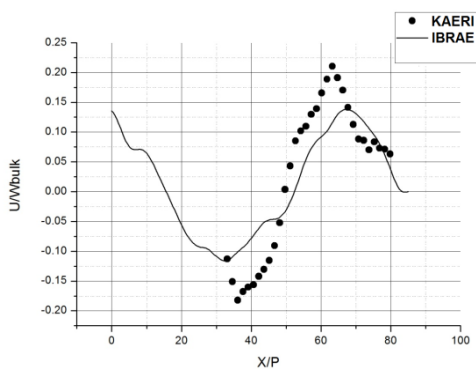


Fig. 9 average U velocity in the cross-section of 4.0 DH in the position y2

As an illustration of the capabilities of the CONV-3d code to estimate the rms characteristics the averaged rms velocity value V in the positions y1 and y2 are presented at figures 10 and 11, correspondingly.

For W-speed processing of experimental results was not conducted carefully enough, as evidenced by the experimenters, therefore, we not shown here this comparison.

On the below at figures 12-19 the results for the cross sections in a sequence of 0.5DH, 1.0 DH, 4.0DH and 10.0DH for grid spacer of swirl-type presents.

Each cross-section contains the results for the y1 and y2 positions.

All results are presented in comparison with data for V component of velocity [9].

In all the figures 12-19 the results of the numerical predictions with the help of CONV-3D code are shown by the solid line.

Experimental data [9] in all figures are shown by dotted line (•••).

As can be seen from figures 12-19, the coincidence with the experiment is good. A discrepancy in values indicates greater uncertainty in the test parameters and, according to the experimenters, needs to be clarified and additional experiments.

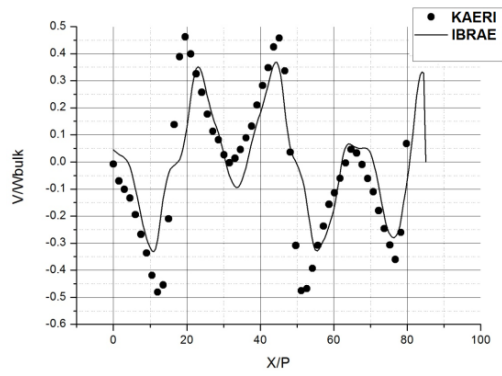


Fig. 12 average V velocity in the cross-section of 0.5 DH in the position y1

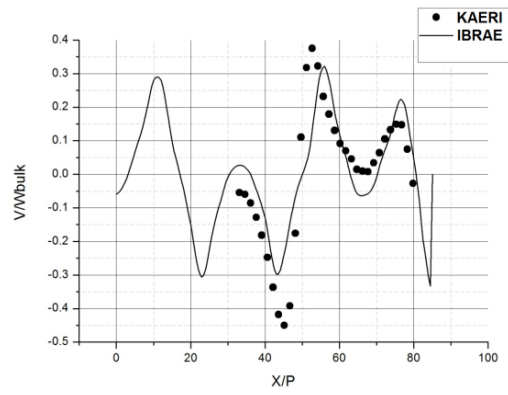


Fig. 15 average V velocity in the cross-section of 1,0DH in the position y2

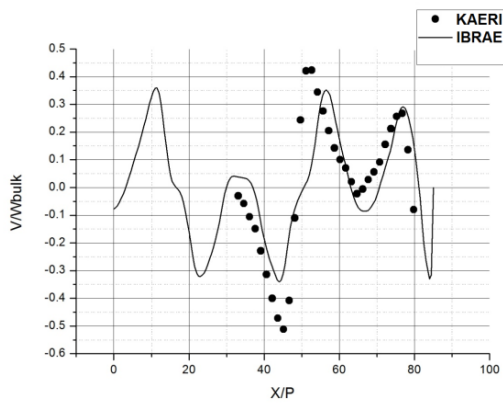


Fig. 13 average V velocity in the cross-section of 0.5 DH in the position y2

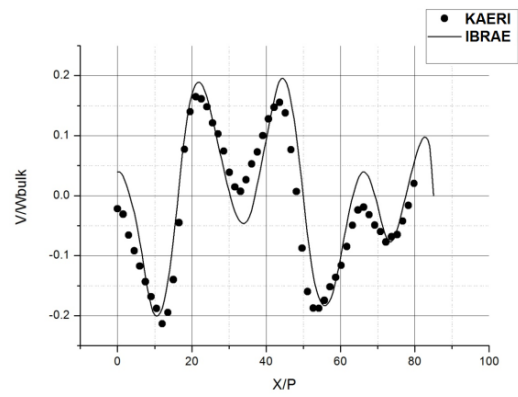


Fig. 16 average V velocity in the cross-section of 4,0DH in the position y1

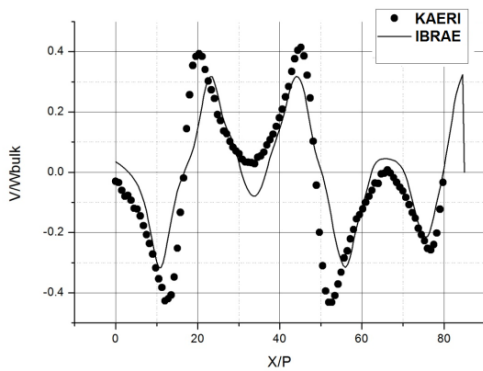


Fig. 14 average V velocity in the cross-section of 1,0DH in the position y1

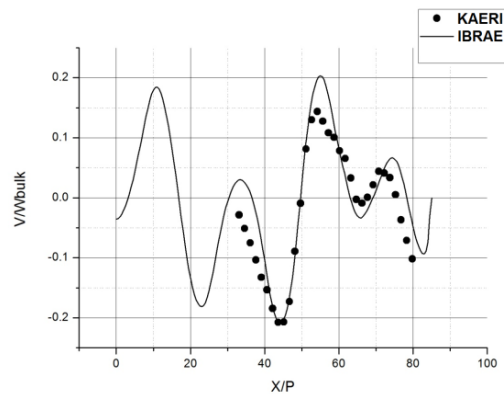


Fig. 17 average V velocity in the cross-section of 4,0DH in the position y2

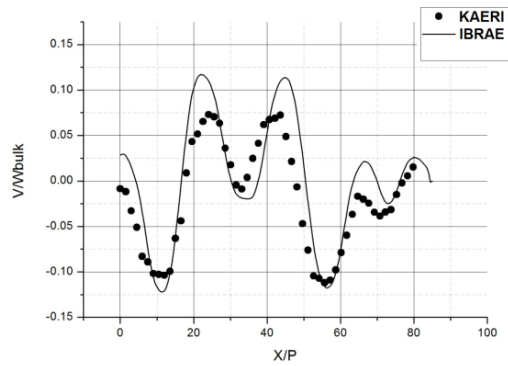


Fig.18 average V velocity in the cross-section of 10,0DH in the position y1

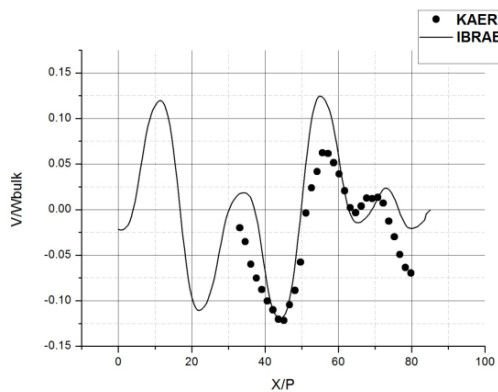


Fig.19 average V velocity in the cross-section of 10,0DH in the position y2

Experimenters conducted the experiment with large errors, and there were many uncertainties in the experiment [9]. Despite this fact, according to the results of the blind test code CONV-3D shared 3-4 place with the code NEK5000 (ANL, USA) among all 20 participants of the blind test [9].

IV. CONCLUSION

The presented results performed allow recommending the use of the CONV-3D code [10] of the DNS class, which has a high predictive capacity, for the calculation water coolant flow around the fuel assembly with different types of grid spacers.

But since the code is written from the first principles, it can be used, without limitation of generality, to solve tasks, in particular, for the reactor facility with sodium coolant, see [11, 12].

Developed DNS CFD code CONV-3D for the simulation of thermal hydraulic processes in fast reactors with liquid metal coolant allows to simulate currents in the structural components of nuclear power plants in a wide range of parameters $Ra < 10^{16}$ and $Re=10^3-10^5$. This is evidenced by

the results of the qualitative and quantitative coincidence with the experiment [11, 12].

REFERENCES

- [1.] S. L. Osipov, et al., "Experience and problems of verification of CFD codes in the projects in the fast reactor", in *Book of abstracts the scientific-technical seminar Problems of verification and application of CFD codes in nuclear engineering*, N. Novgorod, 2012. 62 p.
- [2.] V.V. Chudanov, et al., "A numerical study on natural convection of a heat-generating fluid in rectangular enclosures", *Int. J. Heat Mass Transfer*, 37, 1994, p. 2969.
- [3.] V.V. Chudanov, et al., "Methods of direct numerical simulation of turbulence with use DNS and LES approaches in the tasks of thermal hydraulic fuel Assembly", *Izvestia of Russian Academy of Sciences, Energetics*, 6, 2007, p.47.
- [4.] V.V. Chudanov, et al., "New method for solving of CFD problems at clustered computers petaflops performance". Software systems: theory and applications, 1, 2014, p.3.
- [5.] J. Mahaffy, "Synthesis of Results for the T-junction benchmark", in *Proc. CFD4NRS-3 Conf. on Computational Fluid Dynamics for Nuclear Reactor Safety Applications*, USA, 2010, vol. 1.
- [6.] P. Betts, et al., "Experiments on turbulent natural convection in an enclosed tall cavity", *Int. J. Heat Fluid Flow*, 21, 2000, p.675.
- [7.] B.L. Smith, et al., "Report of the OECD/NEA KAERI Rod Bundle CFD Benchmark Exercise", *Report NEA/OECD, №NEA/CSNI/R(2013)5*, 2013. 124 p.
- [8.] S.K. Chang, S.K. Moon, W.P. Baek, Y.D. Choi, "Phenomenological investigations on the turbulent flow structures in a rod bundle array with mixing devices", *Nucl. Eng. Des.*, 238, 2008, p. 600.
- [9.] H.S. Kang, S.K. Chang, C.-H. Song, "CFD analysis of the MATIS-H experiments on the turbulent flow structures in a rod bundle with mixing vanes", *Proc. CFD4NRS-3*, Washington, D.C., USA, 14-16 September, 2010.
- [10.] V.V. Chudanov, A.E. Aksenova, V.A. Pervichko, A.A. Makarevich, "Supercomputer Mathematical Modeling of the Fluid Dynamics in Elements of Nuclear Power Facilities", *Atomic Energy*, 117(6), 2015, p. 381.
- [11.] V.V. Chudanov, "Development and validation of CONV-3D code for calculation of thermal and hydrodynamics of Fast Reactor at the Supercomputer", *Proc. of an International Conference Fast Reactors and Related Fuel Cycles: Safe Technologies and Sustainable Scenarios (FR13)*, Paris, France, 4-7 March, 2013. Conference ID: 41987 (T1-CN-199).
- [12.] V. Chudanov, et al. "Applications of the DNS CONV-3D Code for Simulations of Liquid Metal Flows", *Proc. International Conference on Fast Reactors and Related Fuel Cycles: Next Generation Nuclear Systems for Sustainable Development*, 26-29 June 2017, Yekaterinburg, RF, p. 229.